On the stability length of fluid/liquid interfaces sustained by microfabricated pillars

J. Berthier, Van Man Tran, H. Jeanson, N. Sarrut
CEA-LETI, Department of Technology for Biology and Health
17, avenue des Martyrs, 38054 Grenoble, France
jean.berthier@cea.fr

ABSTRACT

Extraction of target molecules from a primary liquid and concentration of these molecules in a secondary liquid are now recognized as essential operations before recognition and analysis processes. We focus here on a system constituted of two adjacent microchannels geometrically separated by vertical micro-pillars. The primary and secondary liquids are chosen immiscible, and vertical interfaces attached to the pillars separate the two fluids. The system must be designed to withstand the largest possible interfacial area to favor molecule transfer from primary to secondary fluids. The analysis of the stability of the interface is then the key for the design of the system. In this work, we propose a model for the stability of interfaces attached to circular and lozenge pillars.

Keywords: interface stability, pillars, pinning, transport, molecule transfer.

1 INTRODUCTION

We focus here on the transfer and concentration of macromolecules from a flowing primary carrier fluid to a secondary storage liquid. In the literature such types of concentration microdevices have already been proposed [1]. We analyze the case sketched in figure 1 where the carrier fluid and the storage liquid are flowing side by side, separated by interfaces sustained by micro-pillars. The two immiscible fluids should not mix to form an emulsion, for two reasons: the system should make the economy of a de-mixing system, and on-line detection is facilitated. The best efficiency of such devices is obtained for a largest possible interfacial area. However, it is observed that, for a given geometry of the pillars, there are only a limited number of interfaces that can be stable. In this work, we investigate the stability of the interfaces in function of the geometry (channel length and width, morphology of the pillars) and flow parameters (flow rates in the channels). We deduce an expression for the maximum stability length and we propose some recommendations for improving such a microsystem.

2 MODEL

The two fluids are flowing in parallel with different velocities, and their pressure evolves nearly independently – as long as the interfaces remain stable. Because of the differences of flow rate and geometry, a pressure difference between the two channels builds up. Hence the interfaces are submitted to two constraints: a normal pressure due to the pressure difference between the two channels, and a tangential stress exerted by the friction of the flowing fluids.

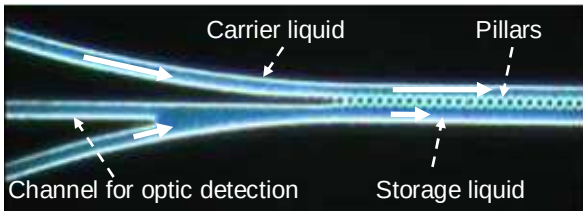

Fig.1. Schematic of the microsystem.

A calculation of the flow with the Comsol numerical software shows that the tangential stress on the interface is much less than the normal stress (fig. 2). Hence, in the following we focus on the normal stress.

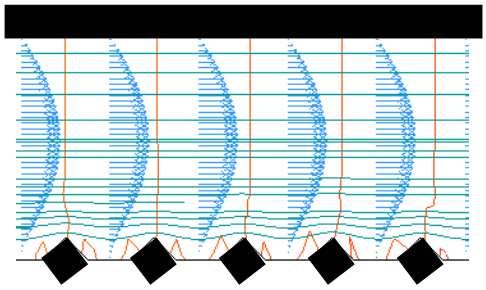

Fig.2. Velocity profile, pressure contour-lines and streamlines in a channel limited by lozenge pillars.

Taking into account the outlet channels (fig. 3), and using the Washburn [2] equation for the pressure drop, modified by the Purday, Shah & London expressions for rectangular channels [3,4], the pressure is function of the distance to the channel entrance, noted x, according to

$$P(x) - P_0 = c\, f(\eta, Q, a, b)\, x + c\, g(\eta, Q, D) \qquad (1)$$

with the notations of figure 3, and where η is the liquid dynamic viscosity. The functions f and g are respectively the pressure drop functions for the "transfer" channel and the outlet channel. The pressure difference across the interface in a cross section of the transfer region is then

$$P_1(x)-P_2(x)=c_1\left[f(\eta_1,Q_1,a_1,b_1)-f(\eta_2,Q_2,a_2,b_2)\right]x + c_2\left[g(\eta_1,Q_1,D_1)-g(\eta_2,Q_2,D_2)\right] \quad (2)$$

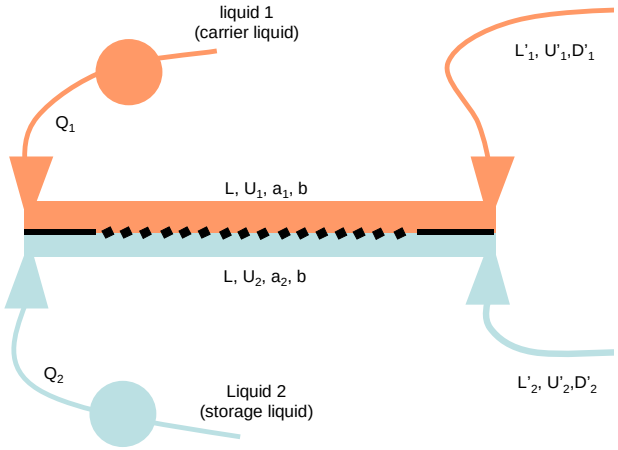

Fig.3. Schematic of the flow parameters.

If we explicit the functions *f* and *g*, equation (2) yields

$$P_1(x)-P_2(x)\cong 8(L-x)\left[\frac{\eta_1 Q_1}{\frac{a_1^3 b^3}{(a_1+b)^2}}-\frac{\eta_2 Q_2}{\frac{a_2^3 b^3}{(a_2+b)^2}}\right] + 32\left(\frac{\eta_1 Q_1 L_1}{\pi D_1^4}-\frac{\eta_2 Q_2 L_2}{\pi D_2^4}\right) \quad (3)$$

If we can determine the maximum pressure difference P_1-P_2 for which an interface remains stable, we obtain the maximum theoretical stability length, sketched in figure 4. The maximum pressure that an interface can withstand has been analyzed analytically and numerically for geometries like lozenges and circles (fig.5). The interface is always anchored to the edges of the lozenge pillars, or satisfies the Young constraints for circular pillars.

a. Lozenge pillars

The stability approach for lozenge pillars is identical to Tsori's approach for wedged pipettes [5], and we will not reproduce the equations here. It suffices to say that the interface is always anchored to the pillar edges. The maximum pressure difference that the interface can sustain (if the pillar edges are perfectly straight) is given by the Laplace equation for a minimum curvature radius

$$\Delta P_{\max}=\frac{\gamma}{R}=\frac{2\gamma}{\delta} \quad (4)$$

where R is the minimum curvature radius and δ the distance between two pillar edges.

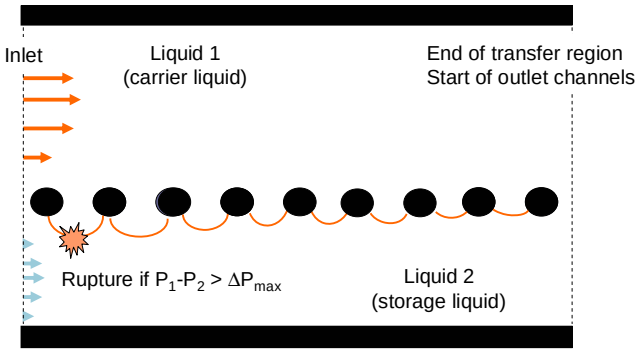

Fig.4. Sketch of the stability of the interfaces. The rupture occurs always at the beginning of the channel (under the condition of perfectly microfabricated pillars).

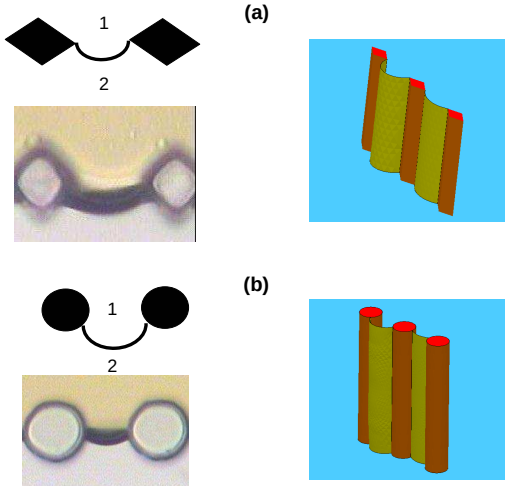

Fig.5. Interface position: (a) the interface is anchored to the pillar edge, (b) the interface adjusts to respect the Young constraint. Experimental photos (left) and Evolver calculation (right) [6].

b. Circular pillars

In this case there is no pinning of the interface; the location of the triple contact line is determined by Young's constraints. Using the notations of figure 6, we locate the position of the contact point M by its angle ϕ, and we have the following relation

$$\frac{h}{2}=r\sin\varphi+R\sin\beta \quad (5)$$

The angle β can be expressed in function of the two angles ϕ and θ by

$$\left(\frac{\pi}{2}-\varphi\right)+(\pi-\beta)+\left(\theta-\frac{\pi}{2}\right)=\pi \quad (6)$$

NSTI-Nanotech 2007, www.nsti.org, ISBN 1420061844 Vol. 3, 2007

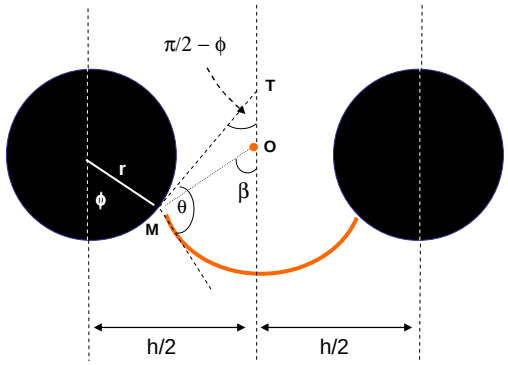

Fig.6. Schematic of the location of the interface. O is the curvature center, T the intersection of the tangent with the median axis, and M the contact point.

And we find

$$\beta = \theta - \varphi \tag{7}$$

Substitution of (7) in (5) produces the curvature radius

$$R = \frac{\frac{h}{2} - r\sin\varphi}{\sin(\theta - \varphi)} \tag{8}$$

The pressure difference across the interface is then

$$\Delta P = \frac{\gamma}{R} = \frac{\gamma \sin(\theta - \varphi)}{\frac{h}{2} - r\sin\varphi} \tag{9}$$

The important point now is to remark that the function $\Delta P(\phi)$ has a maximum; in other words, there is a position of the interface corresponding to a minimum curvature radius, i.e. to a maximum pressure difference. This position is determined by

$$\frac{\partial(\Delta P)}{\partial\varphi} = 0$$

After soma algebra, we find that the solution is given by

$$\varphi_{\max} = \theta - \arccos\left(\frac{2r\sin\theta}{h}\right) \tag{10}$$

And the maximum sustainable pressure is then

$$\Delta P_{\max} = \frac{\gamma \sin(\theta - \varphi_{\max})}{\frac{h}{2} - r\sin\varphi_{\max}} \tag{11}$$

After examination of equations (10) and (11), we deduce that the maximum pressure difference is a function of the Young contact angle θ, the distance between two pillars centers h and the radius of the pillar r.

c. Maximum length

On a general standpoint, the horizontal pressure profiles P_1 and P_2 along the channels are shown in figure 7. According to equations (1) and (3), the profile is piecewise linear, with a jump of the slope between the "transfer" region and the outlet channel.

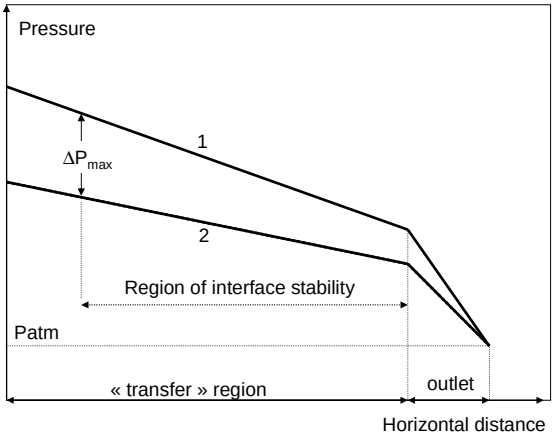

Fig.7. Pressure profiles and determination of the length of interface stability.

Examining the figure, we deduce that there is a maximum stability length corresponding to a pressure difference of ΔP_{max}. Depending on the lozenge or circular geometry, we use equations (4) or (11). Substitution in equation (3) leads to the maximum value of the length of the transfer channel

$$\Lambda = \frac{\Delta P_{\max} - 32\left(\frac{\eta_1 Q_1 L_1}{\pi D_1^4} - \frac{\eta_2 Q_2 L_2}{\pi D_2^4}\right)}{8\left(\frac{\eta_1 Q_1}{\frac{a_1^3 b^3}{(a_1+b)^2}} - \frac{\eta_2 Q_2}{\frac{a_2^3 b^3}{(a_2+b)^2}}\right)} \tag{12}$$

3 EXPERIMENTAL RESULTS

Experiments have been conducted using microfabricated channels of silanized Ordyl. Lozenge and circular pillars (150 µm high) have been tested. Stability has been investigated for water-cyclohexane interfaces.

a. Lozenge pillars

Interfaces attach to the edges of the pillars, as predicted by the theory. When the pressure increases above the rupture threshold or if the edge is not perfectly sharp, the interface

slides along the sides of the pillars and carrier liquid invades the storage channel (fig. 8).

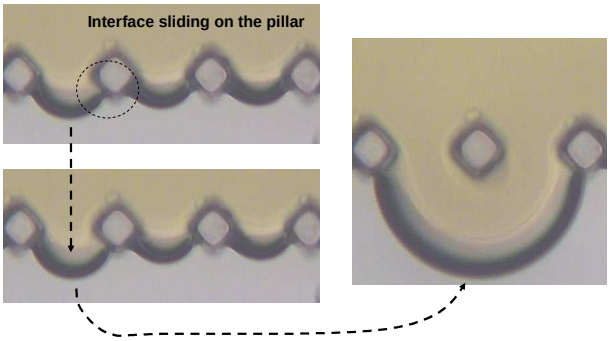

Fig.8. Once the triple contact line has detached from the edge - under the effect of the pressure difference or of a defect in the edge of the pillar – the interface inevitably invades the neighboring channel.

b. Circular pillars

We observe that interfaces take the position predicted by the theory, as shown in figure 9. Above a limit angle ϕ_{max}, the interface is propelled into the other channel.

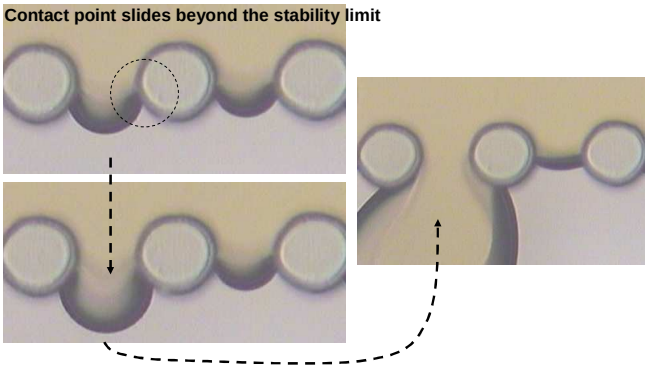

Fig.9. When the pressure difference becomes larger than ΔP_{max}, the contact slides beyond the limit position, the interface invades the neighboring channel.

4 DISCUSSION

Relation (12) shows that, in order to maximize the stability length L_{max}, it is necessary (i) to reduce as much as possible the difference of pressure drop in the outlet channels, (ii) to minimize the pressure drop difference in the transfer region, and (iii) to have the larger possible rupture threshold ΔP_{max}. The rupture threshold ΔP_{max} depends essentially on the free distance between two neighboring pillars, on the interface tension between the two liquids, and on the shape of the pillars. Figure 10 shows a comparison of the rupture pressure threshold between lozenge and circular pillars. Comparison has been performed by considering same exchange surfaces and same free distances between two pillars. The pinning of the interface on the lozenge arêtes stabilizes the interface.

However, the model assumes perfectly microfabricated pillars. In the reality, we have observed that defects on edges deteriorate the pinning of the interface and may lead to a more instable situation. This is the reason why the model somewhat overestimates the stability length.

In conclusion, we can make the following recommendations: The outlet capillary tubes must be carefully designed (length and diameter adapted to the velocities) in order that their specific pressure drop is similar. It is advantageous to have the interfaces attached (pinned) to edges of the vertical pillars. However, if the quality of the edges is not satisfactory, the attachment is poor and sudden break up of the interfaces can take place. The smaller the size of the interfaces, the larger the pressure difference sustained by the interface. Hence, it is advantageous to reduce the size of the interfaces together with the size of the pillars.

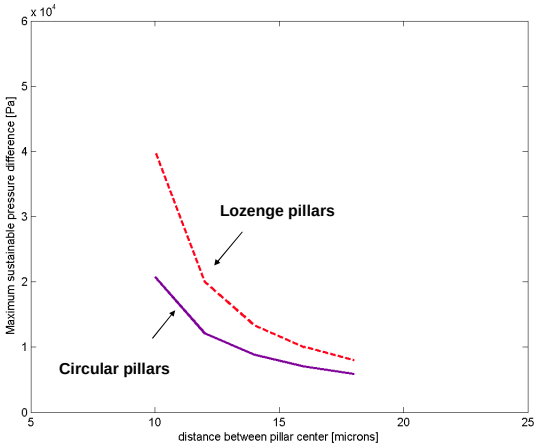

Fig.10. Comparison of stability between lozenge and circular pillars: maximum pressure difference ΔP_{max} versus the distance between pillar centers.

REFERENCES

[1] van der Wijngaart, W., T. Frisk, and G. Stemme, "A micromachined interface for transfer of liquid or vapor sample to a liquid solution," Proceedings of the 13th International Conference on Solid-State Sensors, Actuators and Microsystems, Seoul, June 5-9, 2005

[2] Washburn, E.W., "The dynamics of capillary flow," Phys. Rev., pp. 273-283, 1921

[3] Papautsky, I., B.K. Gale, S. Mohanti, T.A. Ameel, and A.B. Frazier, "Effects of rectangular microchannel aspect ratio on laminar friction constant," Proc. SPIE, Vol. 3877, pp. 147-158, Microfluidic Devices and Systems II,1999

[4] Berthier, J. and P. Silberzan, "Microfluidics for Biotechnology", Artech House, 2005

[5] Tsori, Y., "Discontinuous liquid rise in capillaries with varying cross-sections," Langmuir, 22, pp. 8860-8863, 2006

[6] Brakke, K., "The Surface Evolver," Exp. Math., Vol. 1, 141, 1992